Catalysis Today 147 (2009) 196–202

Contents lists available at ScienceDirect

Catalysis Today

journal homepage: www.elsevier.com/locate/cattod

Methane partial oxidation to synthesis gas over bimetallic cobalt/tungsten carbide catalysts and integration with a Mn substituted hexaaluminate combustion catalyst

Tian-cun Xiao, Ahmad Hanif, Andrew P.E. York [1], Malcolm L.H. Green [*]

Inorganic Chemistry Laboratory, University of Oxford, South Parks Road, Oxford OX1 3QR, UK

ARTICLE INFO

Article history:
Available online 12 July 2009

Keywords:
Methane partial oxidation
Synthesis gas
Stoichiometric total combustion
Metal carbide
Hexaaluminate

ABSTRACT

$Co_{0.2}W_{0.8}C_x$ and supported $Co_{0.2}W_{0.8}C_x$ catalysts are shown to be active for the partial oxidation of methane to synthesis gas. The catalyst stability is improved by operating at elevated pressure, or in the presence of excess methane. At atmospheric pressure the $Co_{0.2}W_{0.8}C_x$ catalysts deactivate by oxidation, as seen by X-ray diffraction. Manganese substituted hexaaluminate catalysts with different Mn contents have been tested as catalysts for the total combustion of methane. In particular $BaMn_2Al_{10}O_{19}$ is active and stable for the combustion reaction. The temperature rise observed in the reactor was up to 300 K, depending on the reaction conditions, and complete conversion of oxygen in the feed was achieved. A process for stabilising the carbide catalysts is demonstrated, combining the manganese substituted hexaaluminate total oxidation catalyst, in series before the carbide reforming catalyst: this process leads to stable operation, with no carbon formation in the reactor and no carbide catalyst oxidation observed.

1. Introduction

In the 1990s Green and co-workers reported that group VI metal carbides, of molybdenum and tungsten, are active catalysts for methane partial oxidation (POM, Eq. (1)), dry reforming and steam reforming [1,2].

$$CH_4 + (1/2)O_2 \rightarrow CO + 2H_2$$
$$\Delta H^{\theta}{}_{298} = -38\ \text{kJ mol}^{-1} \quad \text{partial oxidation} \qquad (1)$$

Catalysts for these reforming reactions are usually based on supported group VIII metals, though the similarity between platinum and tungsten carbide, and ruthenium and molybdenum carbide has been noted before [3,4]. Nevertheless, the observation was surprising since these group VI metal carbides are extremely sensitive to an oxidising atmosphere. The reforming reactions were carried out using stoichiometric feedstocks resulting in product distributions approaching those for the calculated equilibrium. However, the importance of reaction pressure for catalyst stabilisation was emphasised, in particular in the case of methane partial oxidation. LaMont and Thomson investigated the role of pressure in stabilising the catalyst by studying the effect of mass transfer conditions on the stability of Mo_2C for methane dry reforming [5]. It was found that the carbide catalysts are only stable under conditions where the mass transfer coefficient is low, e.g. high pressure and low flow rate, since under these conditions products of the reaction (CO and H_2), which are highly reducing in nature, remain near the catalyst surface, preventing oxidation to take place. In other studies, the methane partial oxidation reaction mechanism over molybdenum carbide has been studied using ^{13}C isotope exchange and *in situ* laser Raman. It appears that the carbon in the lattice of the molybdenum carbide takes an active part in the reaction, while deactivation of the molybdenum carbide catalyst results from the oxidation of the catalyst surface [6,7].

Recently the synthesis and catalytic performance of bimetallic $Co_{0.2}W_{0.8}C_x$ has been reported [8–10]. Here we will show the performance of the $Co_{0.2}W_{0.8}C_x$ material as a catalyst for methane partial oxidation, and also demonstrate the use of a supported $Co_{0.2}W_{0.8}C_x$ catalyst. Furthermore, a two-catalyst system for stabilising the carbide catalysts for POM will be reported, with a total oxidation catalyst, based on a Mn substituted hexaaluminate material, situated in front of the metal carbide reforming catalyst: this process utilizes the knowledge of the POM reaction mechanism, which is generally accepted to proceed first by total oxidation of the methane with oxygen, and then dry and steam reforming of the remaining methane with the CO_2 and H_2O formed in the former reaction. By using the combustion catalyst it is possible to controllably remove all the oxygen from the feed gas before the oxygen sensitive carbide catalyst, and also generate enough heat to efficiently run the carbide reforming catalyst for synthesis gas

* Corresponding author.
E-mail address: malcolm.green@chem.ox.ac.uk (Malcolm L.H. Green).
[1] Current address: Johnson Matthey Technology Centre, Blount's Court, Sonning Common, Reading RG4 9NH, UK.

0920-5861/$ – see front matter © 2009 Elsevier B.V. All rights reserved.
doi:10.1016/j.cattod.2009.05.022

production. Within the study of the integrated system, the performance of different Mn substituted hexaaluminate catalysts under the methane rich feed composition required for POM is also reported.

2. Experimental

2.1. Synthesis of the $Co_{0.2}W_{0.8}C_x$ reforming catalyst

The bulk oxide precursor is prepared using a solid state reaction method, e.g. $Co(NO_3)_2{\cdot}6H_2O$ is ground to mix with WO_3 in a mortar and pestle for 2 h. The mixture was calcined at 650 °C for 4 h, then cooled to room temperature and crushed into a powder. The powder was pressed into pellets, which were calcined at 650 °C for 8 h. The alumina supported catalysts were prepared by mechanically mixing the oxide precursor with the support material.

The carburisation process is the same as that for molybdenum oxide precursors reported previously [8,11]. Briefly, a gas mixture of 10% (in volume) C_2H_6 (10 ml min^{-1}) and 90% H_2 (90 ml min^{-1}) was passed through the oxide precursor material, 1.2 g of $Co_{0.2}W_{0.8}O_x$ in a 4 mm ID quartz tube. The temperature was increased using controlled tubular furnace at a rate of 1 K min^{-1} to 900 K and held until no carbon oxides were detected in the exhaust gas.

2.2. Synthesis of the hexaaluminate combustion catalyst

$BaMn_xAl_{12-x}O_{19}$ samples with nominal composition (x = 0, 1, and 2) have been prepared *via* a co-precipitation method similar to that described previously by Forzatti and coworkers [12,13]. Soluble nitrate salts of the constituents are dissolved in distilled water, and $(NH_4)_2CO_3$ is used as a precipitating agent. The precursor materials were recovered by filtration, washing and overnight drying at 393 K. Calcination was then carried out: temperature programmed calcination from room temperature to 1573 K at a rate of 1 K min^{-1}, followed by a hold at 1573 K for 10 h. The resulting materials were then pulverized, and sieved to 255–350 μm particles for catalytic activity evaluation.

2.3. Catalyst testing and characterisation

Catalytic testing was carried out in a quartz microreactor (ID 8 mm) placed in a tube furnace, with the catalyst material positioned between silica wool plugs within the quartz tube. For measuring the temperature of the catalyst bed, two thermocouples were used: one placed in the outer layer of the silica wool to control the temperature of the furnace and another in the catalyst bed to monitor the temperature change during the combustion. Gas compositions were controlled using mass flow controllers. The products were analyzed by on-line gas chromatography (5880A GC PerkinElmer) equipped with TCD and FID detectors. The X-ray powder diffraction (XRD) patterns of all the samples before and after reaction have been measured using Cu-Kα radiation and a pyrolitic graphite diffracted beam monochromator from 5° to 70°.

3. Results and discussion

3.1. Activity of bulk $CoWC_x$

The results of the $Co_{0.2}W_{0.8}C_x$ activity test for methane partial oxidation to synthesis gas are given in Figs. 1 and 2. This catalyst is active at 830 °C and GHSV of 30,000 h^{-1}, and shows better performance than that of molybdenum carbide published previously [2]. Methane conversion and CO and H_2 selectivity approach the equilibrium values. The ratio of CH_4/O_2 has a large effect on the catalyst activity and selectivity; increasing the CH_4/O_2 improves the catalyst stability and selectivity. However, although the catalyst testing is carried out in a ratio of CH_4/O_2 of 2.7, the reactor is still clean after 100 h running of POM at 830 °C and 4–6 bar, with no carbonaceous material observed on the catalyst. This indicates there is insignificant carbon deposition on the catalyst bed, and that the carbon deposition sometimes seen in the reactor is mainly from the thermal pyrolysis of methane at higher temperature.

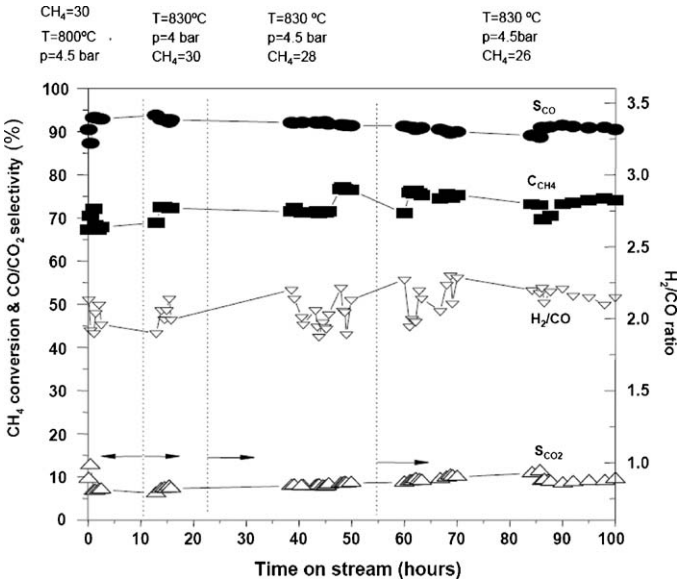

Fig. 1. Methane conversion and product selectivity for partial oxidation over $Co_{0.2}W_{0.8}C_x$ under various conditions as specified in the graph (GHSV: 30,000 ml g_{cat}^{-1} h^{-1}, $CH_4/O_2/N_2$ = 2.6–2.7/1/4).

$Co_{0.2}W_{0.8}C_x$ was also tested at 850 °C and 1 bar (Fig. 2). The methane conversion and CO and H_2 selectivity decrease gradually

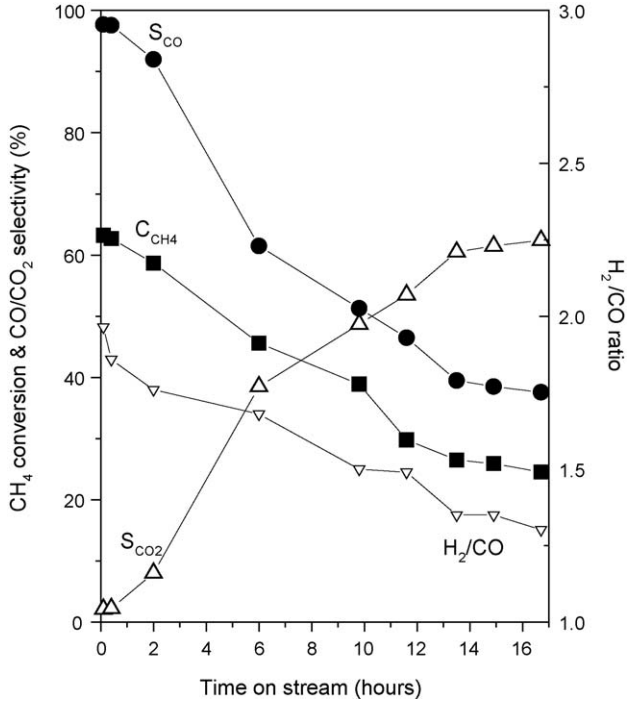

Fig. 2. Methane conversion and product selectivity for partial oxidation over $Co_{0.2}W_{0.8}C_x$ at 850 °C and 1 bar (GHSV: 30,000 ml g_{cat}^{-1} h^{-1}, $CH_4/O_2/N_2$ = 2.6–2.7/1/4).

with time on stream, while carbon dioxide increases. This shows that, as was the case for molybdenum carbide previously, at atmospheric pressure the catalyst is not stable. This again demonstrates the importance of elevated pressure in stabilising the active carbide phase. From these studies it is concluded that the most suitable conditions for POM with the $Co_{0.2}W_{0.8}C_x$ catalyst is around 900 °C, CH_4/O_2 above 2.2 and 6 bar.

Fig. 3 gives the XRD patterns of the $Co_{0.2}W_{0.8}C_x$ before and after POM reaction. For comparison, the pattern for WO_3 (Fig. 3a) and $Co_{0.2}W_{0.8}O_x$ (Fig. 3b) are presented. Before the POM reaction, the as-prepared $Co_{0.2}W_{0.8}C_x$ showed very broad diffraction peaks from 2θ of 35 to 50, with the strong peak at 39.8, which corresponds to W_2C (JCPDS file 653896,W_2C, $P31m$), a sharp diffraction peak at about 44 2θ may be due to the cobalt metal, suggesting that some cobalt may not occupy the lattice of the W_2C.

Fig. 3d is the diffraction pattern of the $Co_{0.2}W_{0.8}C_x$ after POM reaction at 850 °C and 1 bar, which is very similar to the pattern of Fig. 3b, e.g., the $Co_{0.2}W_{0.8}O_x$; this suggests that after the POM reaction at 1 bar and 850°C, the carbide was converted into oxide phase, and the carbide catalyst is not stable under these conditions. However, when the POM reaction is carried out at 830 °C and 5 bar, XRD patterns of the catalyst after reaction showed the main peaks at 2θ of 31.5, 35.8, 48.4, 64.1–65.7, which correspond to WC 0 0 1, 1 0 0, 1 1 0 and 1 1 1 planes (JCPDS file 510939, WC, $P6m2$). This result shows that tungsten carbide changed from W_2C to WC after POM at 830 °C and 4–6 bar. However, no carbon deposition or tungsten oxide is present in the catalyst. This suggests that $Co_{0.2}W_{0.8}C_x$ is stable under these reaction conditions.

The results shown here demonstrate that although bulk Co/W bimetallic carbide shows much better performance than molybdenum carbide in POM to synthesis gas, this material is still prone to deactivation, due to the very oxidising nature of the inlet feed. However, the XRD results also suggest that the structure and pores of Co/W bimetallic carbide are stable and resistant to sintering at high temperature.

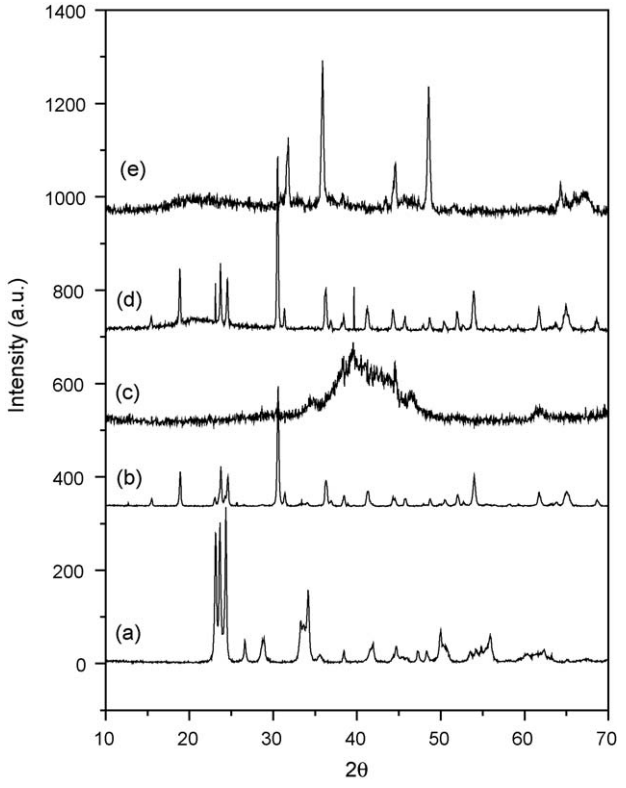

Fig. 3. XRD patterns of $Co_{0.2}W_{0.8}C_x$ before and after reaction: (a) WO_3; (b) $Co_{0.2}W_{0.8}O_x$ carbide precursor; (c) $Co_{0.2}W_{0.8}C_x$ before use; (d) $Co_{0.2}W_{0.8}C_x$ after methane partial oxidation at 850 °C, 1 bar, 24 h; and (e) $Co_{0.2}W_{0.8}C_x$ after methane partial oxidation at 830 °C, 4–6 bar, 100 h.

3.2. Activity of supported $CoWC_x$

Bulk Co/W bimetallic carbide has been demonstrated to be superior in performance for POM than the molybdenum carbide reported previously [2]. In this section the performance of the supported Co/W bimetallic carbide is shown.

The results of the activity test are shown in Fig. 4. It can be seen that the activity of the supported Co/W carbide is not as good as that of the bulk catalyst. The supported catalyst is active and stable for 40 h at 850 °C and high GHSV. The lower activity of supported Co and W bimetallic carbide compared to the bulk carbide is probably due to the presence of less carbide phase for the supported system. After more than 70 h running, no black layer was seen in the reactor wall and also no carbon deposition in the catalyst bed was observed, suggesting that the catalyst is resistant to carbon deposition.

XRD measurement results of the supported bimetallic oxide and carbide are shown in Fig. 5. For comparison, the XRD pattern of as-prepared bulk $Co_{0.2}W_{0.8}O_x$ is presented in Fig. 5a, which shows the typical $CoWO_4$ phase, corresponding to the diffraction peaks at 2θ of 35.6 (2 0 0), 30 (1 1 1), the strongest peak, and 27.5 (1 1 0 and 0 1 1) [14]. When the $Co_{0.2}W_{0.8}O_x$ is mechanically mixed with alumina powder in the presence of alcohol, and calcined at 500 °C, besides the main diffraction pattern of $CoWO_4$, some new peaks at 2θ of 27 and 35 appear, which can be tentatively assigned to WO_2. The carburised $Co_{0.2}W_{0.8}O_x$ showed the main phase of W_2C [15], as described in Fig. 3, although cobalt metal is also present. When $Co_{0.2}W_{0.8}O_x/Al_2O_3$ is carburised to 630 °C with ethane, the XRD pattern (Fig. 5d) is different from that of the bulk supported material; the diffraction peaks at 2θ of 39, 42 and 46 can be assigned to the $Co_6W_6C_x$ carbide [16]. After 30 wt.% $Co_{0.2}W_{0.8}C_x/Al_2O_3$ is used for POM reaction at

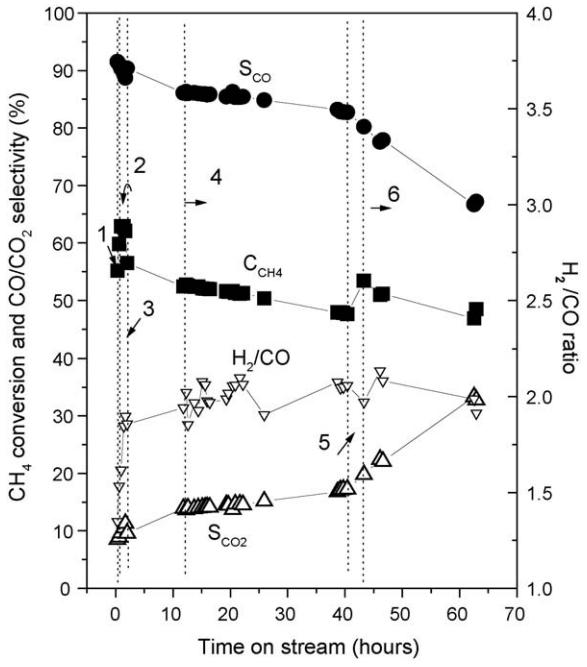

Fig. 4. Methane conversion and product selectivity for partial oxidation over 30 wt.% $Co_{0.2}W_{0.8}C_x/Al_2O_3$: Zone 1: T = 830 °C, p = 4.8 bar, $CH_4/O_2/N_2$ = 30/10/40; Zone 2: T = 850 °C, p = 4.8 bar, $CH_4/O_2/N_2$ = 30/10/40; Zone 3: T = 850 °C, p = 6 bar, $CH_4/O_2/N_2$ = 33/11/44; Zone 4: T = 850 °C, p = 5.5 bar, $CH_4/O_2/N_2$ = 33/11/44; Zone 5: T = 850 °C, p = 6.5 bar, CH_4 = 36, air = 86; Zone 6: T = 850 °C, p = 6.5 bar, $CH_4/O_2/N_2$ = 24/9/36.

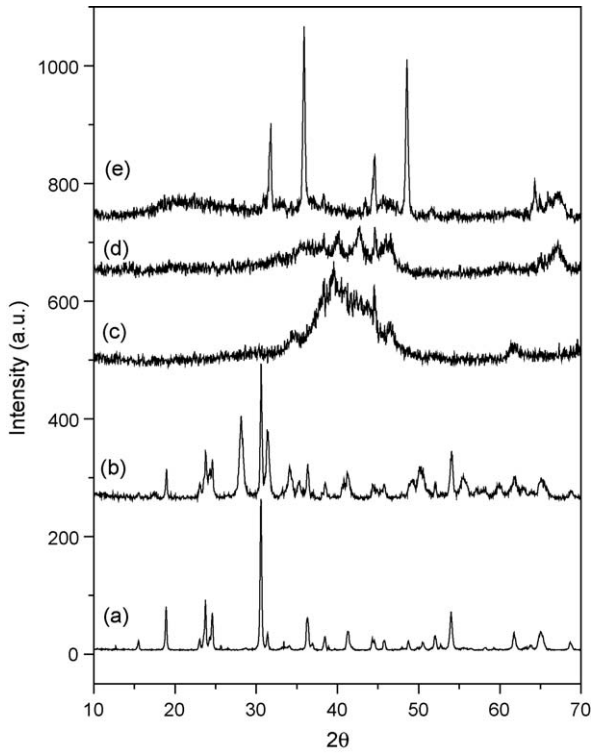

Fig. 5. XRD patterns of the supported Co and W bimetallic oxides and carbides: (a) $Co_{0.2}W_{0.8}O_x$; (b) 30 wt.% $Co_{0.2}W_{0.8}O_x/Al_2O_3$; (c) $Co_{0.2}W_{0.8}C_x$; (d) 30 wt.% $Co_{0.2}W_{0.8}C_x/Al_2O_3$ before use; and (e) 30 wt.% $Co_{0.2}W_{0.8}C_x/Al_2O_3$ after methane partial oxidation at 850 °C, 5–6.5 bar for 60 h.

850 °C, 5–6.5 bar for 60 h a phase transition occurs, with the $C_6W_6C_x$ carbide phase changed to the WC phase. A sharp diffraction peak was seen at 43.9°, which can be assigned to alpha cobalt metal.

Alumina supported Co and W bimetallic carbide has shown good preliminary performance and stability for POM to synthesis gas, though over long test times deactivation is observed. To improve the performance of the catalyst, future work should concentrate on optimizing the catalyst synthesis and studying the effect of different supports.

3.3. Two step process

The catalytic methane partial oxidation reaction route [17] is shown below, and knowledge of this can be used to improve the POM process:

$CH_4 + 2O_2 \rightarrow CO_2 + 2H_2O$ total oxidation

$CH_4 + CO_2 \rightarrow 2CO + 2H_2$ dry reforming

$2CH_4 + 2H_2O \rightarrow 2CO + 6H_2$ steam reforming

$4CH_4 + 2O_2 \rightarrow 4CO + 8H_2$

Initially all the oxygen is consumed in a total oxidation reaction, also removing 25% of the methane from the feed gas. Then the products of total oxidation, namely CO_2 and H_2O, react with the remaining methane, resulting in the overall product distribution expected from POM. This route is well established for the group VIII metal catalysts, e.g. Ni, but evidence also exists that this route is that which occurs with a metal carbide. Fig. 6 shows that, over molybdenum carbide, an exotherm is seen at the front of the

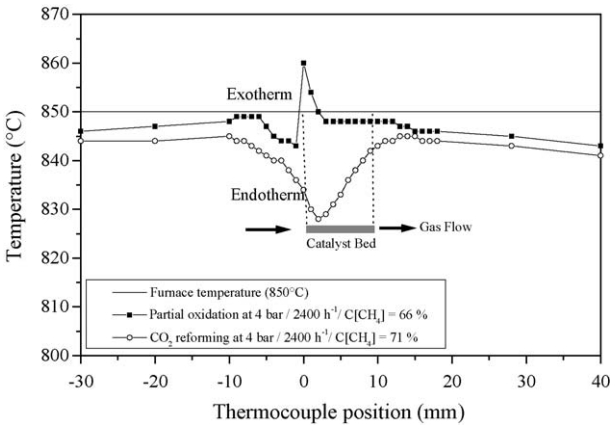

Fig. 6. Temperature profile in the β-Mo_2C/Al_2O_3 catalyst bed.

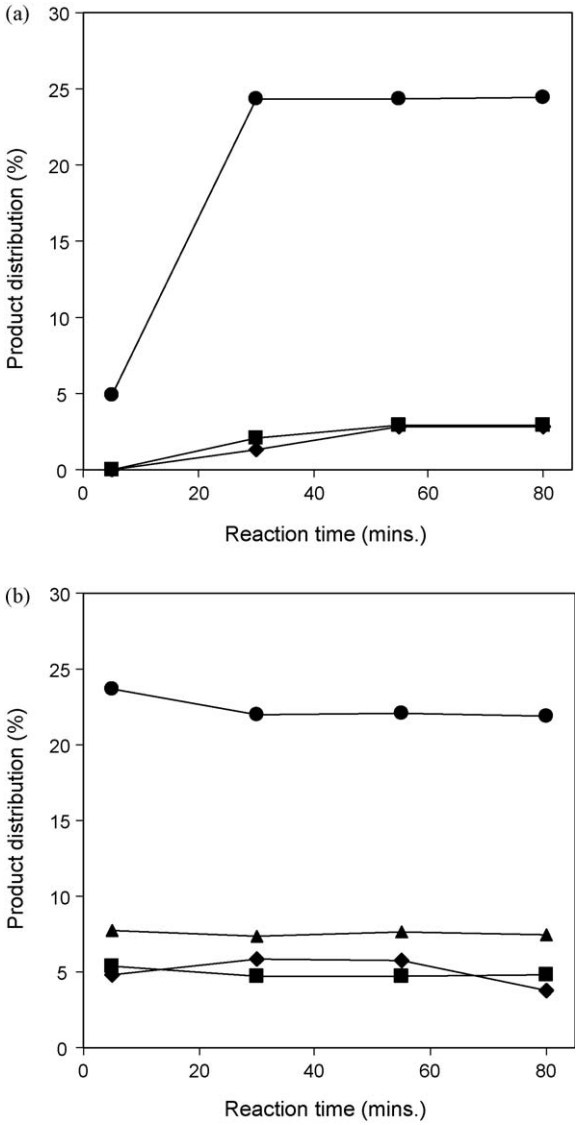

Fig. 7. Product distribution with reaction time of $2CH_4 + O_2$ over $BaMn_2Al_{10}O_{19}$ at (a) 500 °C and (b) 700 °C, at 18,000 h^{-1} (balance is methane); (◆) H_2, (■) CO, (▲) C_2, (●) CO_2.

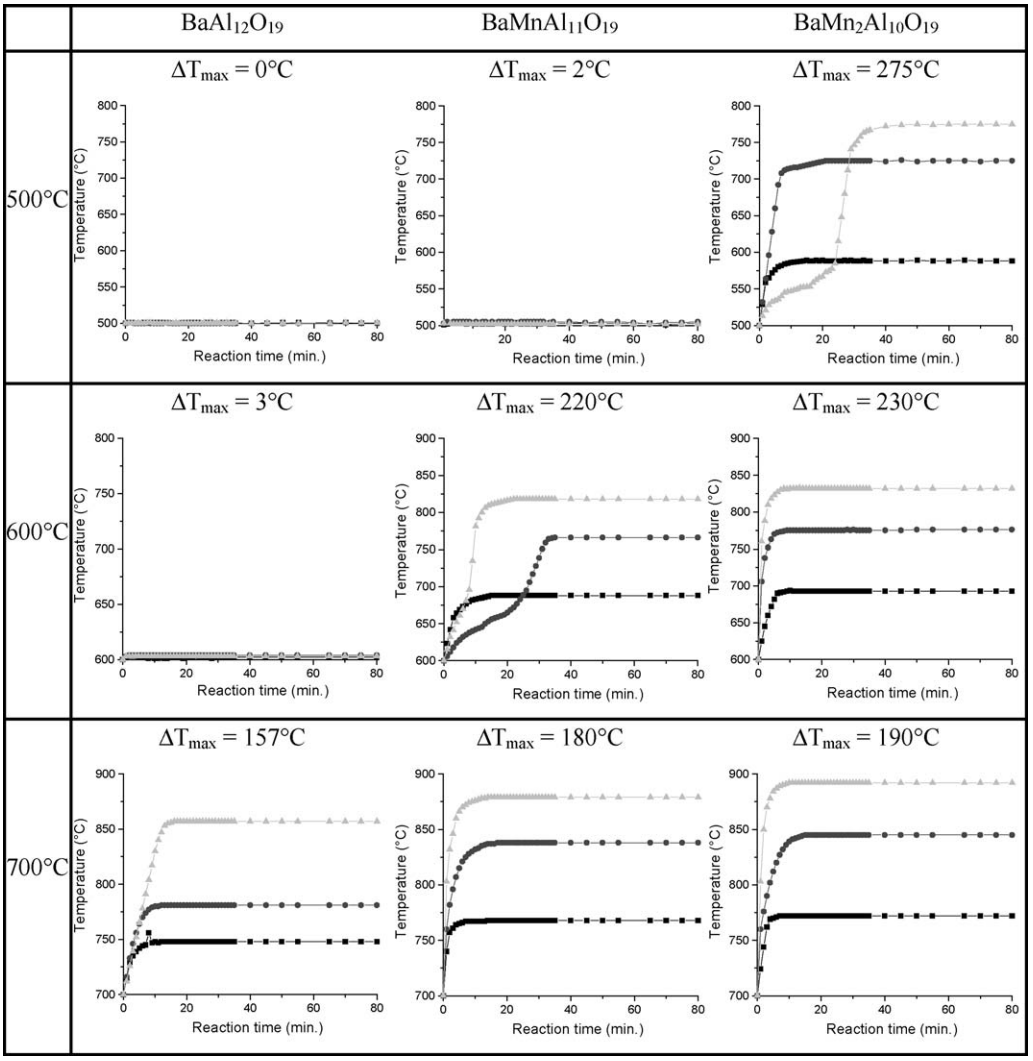

Fig. 8. Temperature change in the catalyst bed during the reaction of $2CH_4 + O_2$ over $BaAl_{12}O_{19}$, $BaMnAl_{11}O_{19}$, and $BaMn_2Al_{10}O_{19}$ at various space velocities and temperatures. ΔT_{max}, maximum exotherm in the experiment for a specific catalyst at a certain temperature. Symbols signify space velocity: squares = 6300 h^{-1}; circles = 12,600 h^{-1}; triangles = 18,000 h^{-1}.

reactor; this is indicative of the exothermic total oxidation reaction. After this initial temperature rise, the temperature of the catalyst drops back to below that of the furnace, indicating an endothermic process: methane steam and dry reforming. The endothermicity of dry reforming is also shown in Fig. 6 for comparison. It should be possible to use knowledge of the POM reaction route to design a process to remove all the oxygen from the feed gas over a very stable catalyst, in terms of sensitivity to oxygen, carbon formation in the pre-catalytic zone and sintering due to the exothermic reaction taking place. The catalyst exotherm over the total oxidation catalyst can also be used to raise the reactor to a temperature more suitable for methane reforming (e.g. >850 °C).

The proposed process, using two catalysts in series, incorporates a manganese substituted barium aluminate catalyst, which have been identified as suitable candidates for the total oxidation reaction [18].

3.3.1. Mn substituted hexaaluminates for methane combustion

Manganese substituted barium aluminate catalysts, $BaAl_{12}O_{19}$, $BaMnAl_{11}O_{19}$ and $BaMn_2Al_{10}O_{19}$, have been studied for the methane rich combustion reaction, with a feedstock comprising methane and oxygen in the ratio 2:1, i.e. the ideal ratio for POM.

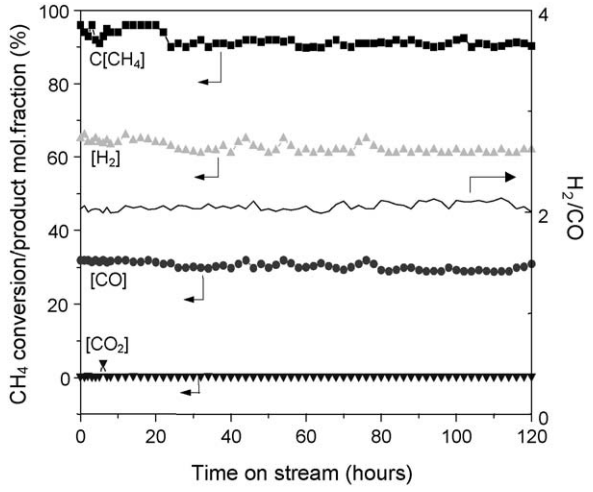

Fig. 9. Methane conversion and product mole fraction for the partial oxidation process incorporating a $BaMn_2Al_{10}O_{19}$ oxidation catalyst in series with the $CoWC_x$ reforming catalyst (850 °C, 1 bar).

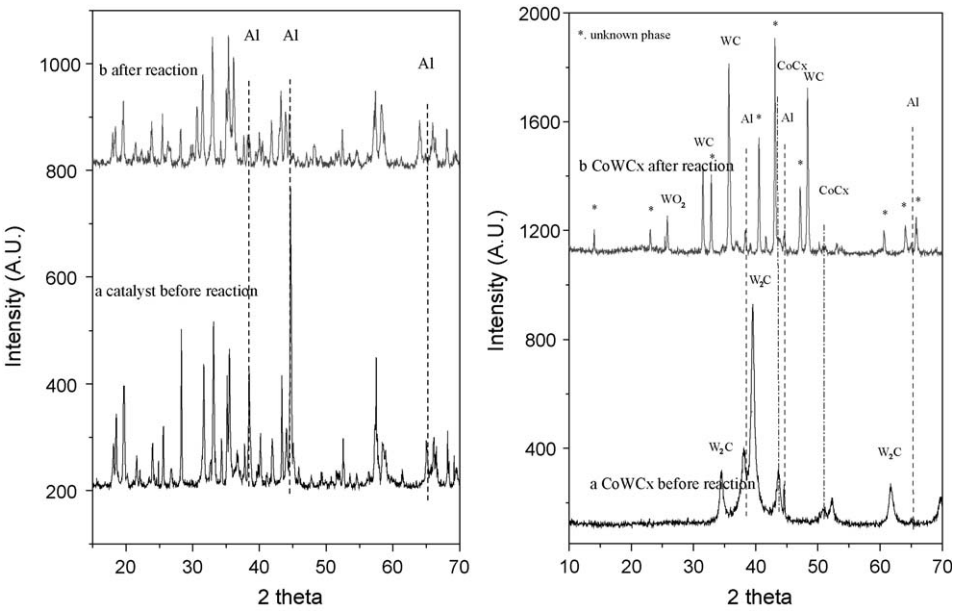

Fig. 10. XRD patterns of the $BaMn_2Al_{10}O_{19}$ combustion catalyst (left side) and the $CoWC_x$ methane reforming catalyst (right side), before use and after methane partial oxidation for 120 h.

The temperature profile of the catalyst bed has been monitored, along with the reaction products. The aim is to achieve high catalyst activity for total oxidation, and also a high catalyst exotherm to pass on to the reforming catalyst. The results are shown in Figs. 7 and 8.

In Fig. 7 it can be seen that using $BaMn_2Al_{10}O_{19}$, the theoretical maximum methane conversion under these conditions, i.e. 25%, has been achieved, since the distribution of the products is dominated by carbon dioxide (almost 25%), and this is even possible at 500 °C. The products are those expected for the total oxidation reaction. Furthermore, it can be seen from Fig. 8 that the exotherm generated over the $BaMn_2Al_{10}O_{19}$, catalyst can be 200–300 °C, depending on reaction temperature. The reaction can be expressed as follows:

$$2CH_4 + O_2 = 1.5CH_4 + (1/2)CO_2 + H_2O$$

Increased conversion of O_2 will give more heat, and if the above reaction in the presence of O_2 is complete combustion, theoretical CH_4 conversion should be 25%. When less combustion reaction occurs, less heat would be generated from the combustion reaction, thus the temperature rise would be lower.

Fig. 8 shows that lower exotherms were observed over the $BaAl_{12}O_{19}$ and $BaMnAl_{11}O_{19}$ materials, showing that the relative activity for these materials under the POM reaction conditions is: $BaMn_2Al_{10}O_{19} > BaMnAl_{11}O_{19} > BaAl_{12}O_{19}$. The less active catalysts also produced total oxidation products, but with lower selectivity, and ethene and ethane, from methane oxidative coupling, were also observed, resulting in the lower exotherms; this is not surprising given that the methane/oxygen feed ratio is ideal for oxidative coupling, while also limiting the extent of total oxidation.

Therefore the most suitable catalyst for integration into the combined process is $BaMn_2Al_{10}O_{19}$.

3.3.2. Integration of the combustion and reforming catalysts

The integrated process was carried out by placing the two catalysts in series in the reactor. The reaction conditions were 1 bar, 850 °C, pre-reforming catalyst: 0.2 g $BaMn_2Al_{10}O_{19}$, reforming catalyst: 0.3 g, methane flow rate: 11 ml min^{-1}, O_2 flow rate: 5.0 ml min^{-1}. Fig. 9 shows that the POM performance of the two catalysts in series is very good; after 5 days continuous operation, the catalyst is still very stable and active. This is in contrast to the performance of the $Co_{0.2}W_{0.8}C_x$ catalyst without the pre-oxidation catalyst in series; it has been shown here and previously [6] that deactivation can occur very quickly for these catalysts in POM. In the combined process, the conversion of methane over $CoWC_x$ is above 90%, and the ratio of H_2 to CO is almost always above 2. Almost no carbon deposits were found in the reactor.

Fig. 10 shows the XRD measurements of the combustion and reforming catalysts, before and after reaction. The structure of the combustion catalyst is maintained after 5 days reaction, as shown in Fig. 10 (left), the overall diffraction pattern of the catalyst is almost unchanged. However, the crystallinity of the catalyst is a little lower, as reflected by the lower diffraction intensity, suggesting the particle size is becoming finer.

Fig. 10 (right) shows the XRD pattern of the $CoWC_x$ catalyst before and after POM reaction at 850 °C, and 1 bar for 120 h. It is seen that the main phase of the as-prepared carbide is W_2C before the reaction. After the POM reaction, structure of the reforming catalyst changed, the tungsten carbide transformed into WC and $Co_6W_6C_x$, while the catalyst was still active after 5 days reaction. The phase transformation is probably caused by the high temperature treatment, because the carbide was originally prepared at a temperature lower than 700 °C. There is also trace amount of WO_2, and some cobalt exists as metal after reaction. Despite this, the catalyst remains stable under the reaction atmosphere.

Integration of combustion and reforming processes may offer a route for prolonging the lifetime of the carbide catalysts, mainly due to removal of oxygen before the carbide catalyst. Manganese substituted hexaaluminate is a good candidate for the total oxidation catalyst.

4. Conclusions

It has been shown that the performance of the group VI metal carbides for methane partial oxidation to synthesis gas can be improved by using bimetallic materials, either in bulk form or supported. $Co_{0.2}W_{0.8}C_x$ and supported $Co_{0.2}W_{0.8}C_x$ catalysts are both active for POM, and also very stable at elevated pressures. At

atmospheric pressure deactivation by oxidation is observed, however, a two-catalyst process has been demonstrated that improves the stability of the catalysts for the POM process even at atmospheric pressure. $BaMn_2Al_{10}O_{19}$ is an excellent candidate for methane total combustion under POM conditions, with high exotherms achievable over the catalyst: this heat can be used downstream in the reforming catalyst bed. When the $BaMn_2Al_{10}O_{19}$ is placed in series with the $Co_{0.2}W_{0.8}C_x$ catalyst, the overall methane oxidation process performance is stable for 5 days. No carbon formation in the reactor and no carbide catalyst oxidation was observed. The high stability of the reforming catalyst probably results from the pre-combustion of methane with oxygen, thus removing oxygen before the carbide catalyst: the carbide catalyst only catalyses dry and steam reforming reactions in this process.

References

[1] A.P.E. York, J.B. Claridge, A.J. Brungs, S.C. Tsang, M.L.H. Green, Chem. Commun. (1997) 39.
[2] J.B. Claridge, A.P.E. York, C. Márquez-Alvarez, A.J. Brungs, J. Sloan, S.C. Tsang, M.L.H. Green, J. Catal. 180 (1998) 85–100.
[3] J.M. Muller, F.G. Gault, Bull. Soc. Chim. Fran. 2 (1970) 416.
[4] R.B. Levy, M. Boudart, Science 181 (1973) 547.
[5] D.C. LaMont, W.J. Thomson, Appl. Catal. A: Gen. 274 (2004) 173.
[6] T.C. Xiao, A. Hanif, A.P.E. York, Y. Nishizaka, M.L.H. Green, Phys. Chem. Chem. Phys. 4 (2002) 4549.
[7] D.C. LaMont, W.J. Thomson, Chem. Eng. Sci. 60 (2005) 3553.
[8] T.-C. Xiao, A.P.E. York, H. Al-Megren, V.C. Williams, H.-T. Wang, M.L.H. Green, J. Catal. 202 (2001) 100.
[9] M.L.H. Green, T.-C. Xiao, US Patent 7,183,329, February 27, 2007.
[10] T.-C. Xiao, A.P.E. York, H. Al-Megren, V.C. Williams, H.-T. Wang, M.L.H. Green, C. R. Acad. Sci. Ser. IIc 3 (2000) 451.
[11] J.B. Claridge, A.P.E. York, A.J. Brungs, M.L.H. Green, Chem. Mater. 12 (2000) 132.
[12] G. Groppi, M. Bellotto, C. Cristiani, P. Forzatti, P.L. Villa, Appl. Catal. A: Gen. 104 (1993) 101.
[13] M. Bellotto, G. Artioli, C. Cristiani, P. Forzatti, G. Groppi, J. Catal. 179 (1998) 597.
[14] L. Zhen, W.-S. Wang, C.-Y. Xu, W.-Z. Shao, L.-C. Qin, Mater. Lett. 62 (2008) 1740.
[15] A.S. Kurlov, A.A. Rempel, Inorg. Mater. 43 (2007) 602.
[16] P. Peetsalu, S. Zimakov, J. Pirso, V. Mikli, R. Tarbe, P. Kulu, Proc. Eston. Acad. Sci. Eng. 12 (2006) 435.
[17] A.P.E. York, T.-C. Xiao, M.L.H. Green, J.B. Claridge, Catal. Rev. 49 (2007) 511.
[18] V. Pitchon, D.Y. Murzin, Chem. Eng. Technol. 24 (2001) 1301.